Functional comparison of Fc-engineering strategies to improve anti-HIV-1 antibody effector functions

Schriek, A.I.; Falck, D.; Wuhrer, M.; Kootstra, N.A.; Gils, M.J. van; Taeye, S.W. de

Antiviral Research 231 (2024) 106015

Contents lists available at ScienceDirect

Antiviral Research

journal homepage: www.elsevier.com/locate/antiviral

Functional comparison of Fc-engineering strategies to improve anti-HIV-1 antibody effector functions

Angela I. Schriek [a,b,*], David Falck [c], Manfred Wuhrer [c], Neeltje A. Kootstra [b,d], Marit J. van Gils [a,b], Steven W. de Taeye [a,b,**]

[a] Amsterdam UMC location University of Amsterdam, Department of Medical Microbiology, Amsterdam, the Netherlands
[b] Amsterdam Institute for Infection and Immunity, Infectious diseases, Amsterdam, the Netherlands
[c] Center for Proteomics and Metabolomics, Leiden University Medical Center, Leiden, the Netherlands
[d] Amsterdam UMC location University of Amsterdam, Department of Experimental Immunology, Amsterdam, the Netherlands

ARTICLE INFO

Keywords:
Broadly neutralizing antibodies
HIV-1 cure
Antibody engineering
Antibody-dependent cellular phagocytosis
Antibody-dependent cellular cytotoxicity

ABSTRACT

Substantial reduction of the intact proviral reservoir is essential towards HIV-1 cure. *In vivo* administration of broadly neutralizing antibodies (bNAbs) targeting the HIV-1 envelope glycoprotein (Env) trimer can decrease the viral reservoir, through Fc-mediated killing of infected cells. In this study, we compared three commonly used antibody engineering strategies to enhance Fc-mediated effector functions: (i) glyco-engineering, (ii) protein engineering, and (iii) subclass/hinge modifications in a panel of anti-HIV-1 antibodies. We found that antibody-dependent cellular phagocytosis (ADCP) was improved by elongating the hinge domain and switching to an IgG3 constant domain. In addition, potent NK cell activation and ADCC activity was observed for afucosylated antibodies and antibodies bearing the GASDALIE mutations. The combination of these engineering strategies further increased NK cell activation and induced antibody dependent cytotoxicity (ADCC) of infected cells at low antibody concentrations. The bNAb N6 was most effective at killing HIV-1 infected cells, likely due to its high affinity and optimal angle of approach. Overall, the findings of this study are applicable to other antibody formats, and can aid the development of effective immunotherapies and antibody-based treatments for HIV-1 cure strategies.

1. Introduction

HIV-1 continues to be a significant global health problem, affecting approximately 39.0 million individuals worldwide. While tremendous progress has been made in treating HIV-1 infection with antiretroviral therapy (ART), a cure remains elusive (Gulick et al., 1997; Hammer et al., 1997). HIV-1 has the unique ability to integrate its genetic material into the host's immune cells, establishing long-lasting reservoirs (Pierson et al., 2000; Smith et al., 2006; Wagner et al., 2014; Maldarelli et al., 2014). These reservoirs pose a significant barrier to achieving a cure, and cells harboring an intact HIV-1 provirus can produce infectious virus when ART is discontinued. To reach a state of cure, a substantial reduction of the viral reservoir is essential (Hill et al., 2014; Busman-Sahay et al., 2021). Therefore, efforts to eradicate HIV-1 infected cells to reduce the viral reservoir are of interest, including the use of broadly neutralizing antibodies (bNAbs).

Approximately 2–3 years after an acute HIV-1 infection, 20–50% of people with HIV-1 develop bNAbs. These bNAbs recognize conserved regions of the HIV-1 envelope glycoprotein (Env) on infected cells and virions, and exhibit the capacity to neutralize the majority of circulating viral strains effectively (Sok et al., 2018; Freund et al., 2017; Gray et al., 2011; Hraber et al., 2014; Scheid et al., 2009). The bNAb antigen-binding site recognizes various conserved epitopes on Env, including the variable loop 3 base and glycans (V3 glycan; e.g., PGT121), Env trimer apex (e.g., PGDM1400), gp41 membrane proximal region (MPER), CD4-binding site (CD4bs; e.g., VRC01 and N6), gp120-gp41 subunit interface, gp120 silent face, and fusion peptides (Sok et al., 2018; Caskey, 2020; Liu et al., 2020a; Kumar et al., 2023).

Recent human clinical trials have demonstrated the effectiveness of broadly neutralizing antibodies (bNAbs) targeting HIV-1 Env in maintaining viral suppression and reducing the risk of viral escape when employed as a combination therapy approach with multiple bNAbs

* Corresponding author. Amsterdam UMC location University of Amsterdam, Department of Medical Microbiology, Amsterdam, the Netherlands.
** Corresponding author. Amsterdam UMC location University of Amsterdam, Department of Medical Microbiology, Amsterdam, the Netherlands.
E-mail addresses: a.i.schriek@amsterdamumc.nl (A.I. Schriek), s.w.detaeye@amsterdamumc.nl (S.W. de Taeye).

https://doi.org/10.1016/j.antiviral.2024.106015
Received 12 July 2024; Received in revised form 17 September 2024; Accepted 25 September 2024
Available online 27 September 2024

(Klein et al., 2012; Barouch et al., 2013; Shingai et al., 2013; Nishimura et al., 2017). Administering bNAbs at the initiation of ART has also shown promise in inducing CD8-mediated control (Borducchi et al., 2018; Mendoza et al., 2018; Niessl et al., 2020; Gaebler et al., 2022; Rosás-Umbert et al., 2022; Sneller et al., 2022). Through the binding of the Fc domain to activating Fc gamma receptors (FcγRs) on immune cells, bNAbs facilitate Fc-mediated effector functions such as antibody-dependent cellular phagocytosis (ADCP) and antibody-dependent cellular cytotoxicity (ADCC) that enable the elimination of HIV-1 infected cells *in vivo* (Hayes et al., 2014; Flerin et al., 2019; Halper-Stromberg et al., 2014; Lu et al., 2016; Horwitz et al., 2013; Schoofs et al., 2016). Among the various antibody effector functions, ADCC has been predominantly correlated with a reduction in the viral reservoir size (Marchitto et al., 2023; Suryawanshi et al., 2021; Bruel et al., 2016; Flórez-Álvarez et al., 2018; Guo et al., 2022), suggesting that natural killer (NK) cells may represent a promising target for an HIV-1 cure. This observation is consistent with findings from studies involving elite controllers (ECs) and people with HIV-1 (PWH), which have demonstrated an inverse correlation between NK cell activity and cytotoxicity and HIV-1 DNA levels (Etemad et al., 2023; Hartana et al., 2022, 2023; Olesen et al., 2015; Utay et al., 2020; Hua et al., 2018). Additionally, in a recent clinical study, the administration of the bNAbs 3BNC117 and 10–1074 led to a decrease in the size of the intact proviral reservoir (Gaebler et al., 2022). These collective findings underscore the potential of antibody-based therapies to advance HIV-1 cure strategies.

The elimination of viral reservoir cells by bNAbs *in vivo* is hampered by the low Env density on reservoir cells, immune cell exhaustion in PWH, viral escape, and antibody half-life (Amitai et al., 2018; Fuller et al., 2004; Zhao et al., 2022; Vidarsson et al., 2014). Next-generation engineered bNAbs that overcome these limitations are of great interest for future HIV-1 cure strategies (Schriek et al., 2023). Antibody Fc-engineering is one of the strategies that could be used to overcome the limitations. Antibody engineering aims to modify the properties of antibodies, including increasing the affinity for the target antigen, improving Fc-mediated effector functions, prolonging *in vivo* half-life and/or reducing immunogenicity (Mackness et al., 2019; Saxena et al., 2016). Strategies that aim to improve Fc effector functions focus on enhancing the interaction between the Fc domain and Fc gamma receptors (FcγRs) on immune cells, thereby leading to increased clearance of infected cells. Three engineering strategies, namely glyco-engineering, protein engineering, and subclass/hinge modifications, are frequently explored in research concerning anti-HIV-1 bNAbs. Glyco-engineering involves modifying the sugar molecules attached to the Fc domain, enhancing the antibody's interaction with immune cells. A common approach is the removal of core fucose from the IgG Fc region, which significantly increases antibody binding affinity to FcγRIIIa on NK cells, thereby enhancing ADCC activity (Niwa et al., 2004; Ferrara et al., 2011; Liu et al., 2015; de Taeye et al., 2024). Protein engineering focuses on introducing specific point mutations within the Fc domain of the antibody to optimize its binding to FcγRs. For instance, mutations such as G236A and DE (S239D/I332E) in the CH2 region have been shown to significantly increase affinity for FcγRIIa and FcγRIIIa, consequently boosting effector functions such as ADCC and ADCP (Lazar et al., 2006; Richards et al., 2008; Liu et al., 2020b; Stavenhagen et al., 2007). The combination of these mutations; GASDALIE (G236A/S239D/A330L/I332E) synergistically improved affinity to FcγRIIa and FcγRIIIa, enhancing ADCC and ADCP (Ahmed et al., 2016). Conversely, antibodies bearing LALA (L234A/L235A) or PGLALA (L234A/L235A/P329G) mutations have reduced binding to FcγRs, minimizing effector functions and complement activity, while preserving neonatal Fc receptor (FcRn) binding (Damelang et al., 2024; Schlothauer et al., 2016). Lastly, modifying the antibody's subclass or hinge region—for example, transitioning from a standardized IgG1 to an IgG3—can significantly enhance its functional properties, including ADCP and ADCC activities (Saxena et al., 2016; Chu et al., 2020; Richardson et al., 2019, 2021; De Taeye et al., 2020). Incorporating longer, more flexible hinge regions, such as those from IgG3 or camelid antibodies, has been shown to boost ADCC and improve neutralization potency (Moyo-Gwete et al., 2022; D'Eall et al., 2019; Foss et al., 2022). Overall, these Fc engineering strategies have the potential to enhance the antiviral properties of anti-HIV-1 antibodies, making them viable candidates for curative strategies.

No study has yet compared all three types of engineering strategies in a single comprehensive study, evaluating their impact on various antibody effector functions and functional killing assays. In this study, we applied the three commonly used Fc engineering strategies to a panel of anti-HIV-1 antibodies (PGDM1400, PGT121, N6, A32) and nanobody-IgG1 constructs (J3 and 1F10) targeting various epitopes on the HIV-1 Env trimer. We found that longer hinge length and IgG3 subclass backbone improves FcγRIIa binding and ADCP, while afucosylated and GASDALIE (G326A/S239D/A330L/I332E) antibody variants enhanced FcγRIIIa binding and NK cell activation. Combining the latter engineering strategies further improved NK cell activation and ADCC activity. In summary, this study highlights the potential of various Fc engineering strategies to enhance the capacity of antibodies to induce Fc-mediated effector functions and eliminate HIV-1 reservoir cells, which may prove to be valuable for HIV-1 cure strategies.

2. Results

2.1. Characterization of Fc-engineered anti-HIV-1 antibodies

To study the effect of Fc engineering strategies in an HIV-1 context, we selected six anti-HIV-1 antibodies with varying breadth, potency and epitope: We picked broadly neutralizing antibodies PGDM1400 (V2-Apex), PGT121 (V3-glycan super site), N6 (CD4 binding site (CD4bs)) and a non-neutralizing antibody A32 (Cluster A inner domain) (A32). In addition, we selected two nanobody-IgG1 constructs targeting the CD4bs (J3) and V3 loop (1F10). The antibodies were produced in seven different formats: IgG1*01, IgG3*01, IgG1*01 Fc domain variants coupled with either an IgG3 hinge (62 amino acids; IgG1 IgG3 hinge) or a camelid IgG2 hinge (35 amino acids; IgG1 Camelid hinge), an afucosylated IgG1 antibody, an IgG1 bearing the GASDALIE (G326A/S239D/A330L/I332E) mutations, and a control Fc-dead IgG1 antibody bearing the PGLALA (L234A/L235A/P329G) mutations (Fig. 1A). The antibodies were produced in HEK293F cells. SDS page and ELISA confirmed that the antibody integrity and antigen binding (BG505 SOSIP or BG505 gp120) were not compromised by altered glycosylation, hinge engineering or Fc mutagenesis (Sup Fig. 2A–C). The antibodies migrated according to their expected molecular weights, allowing for the clear identification of hinge-engineered variants due to the presence of a higher HC band in the gel. Additionally, antibodies with an IgG3 hinge displayed a more heterogeneous HC size, likely due to variations in O-glycosylation (Plomp et al., 2015). Furthermore, antibodies produced in the presence of 2-fluorofucose (2FF) showed a significant reduction in fucosylation levels, decreasing from approximately 98% to 10–20% (Sup Fig. 2D).

We characterized neutralization capacity of all Fc-engineered variants, as previous studies demonstrated that switching to an IgG3*01 subclass or hinge can enhance neutralization capacity (Richardson et al., 2019; Moyo-Gwete et al., 2022). We occasionally observed a slight, antibody- and virus-specific enhancement in neutralization for IgG3 and extended hinge variants (Sup Fig. 3A and B), consistent with prior findings. All other engineered variants displayed similar neutralization capacity as compared to their IgG1 counterparts (Sup Fig. 3C and D).

Next, we determined the binding strength of the Fc engineered antibodies to FcγRIIa (Fig. 1B) and FcγRIIIa (Fig. 1C) in ELISA in an antigen bound setting, either BG505 SOSIP (PGDM1400, PGT121, N6, and J3) or BG505 gp120 (A32 and 1F10). Antibody variants with GASDALIE mutations exhibited a significant increase in binding to FcγRIIa (2.3-fold) and FcγRIIIa (5.4-fold) compared to IgG1 counterparts (Fig. 1D and E and Sup Fig. 4). IgG3 hinge and full IgG3 antibodies showed a modest

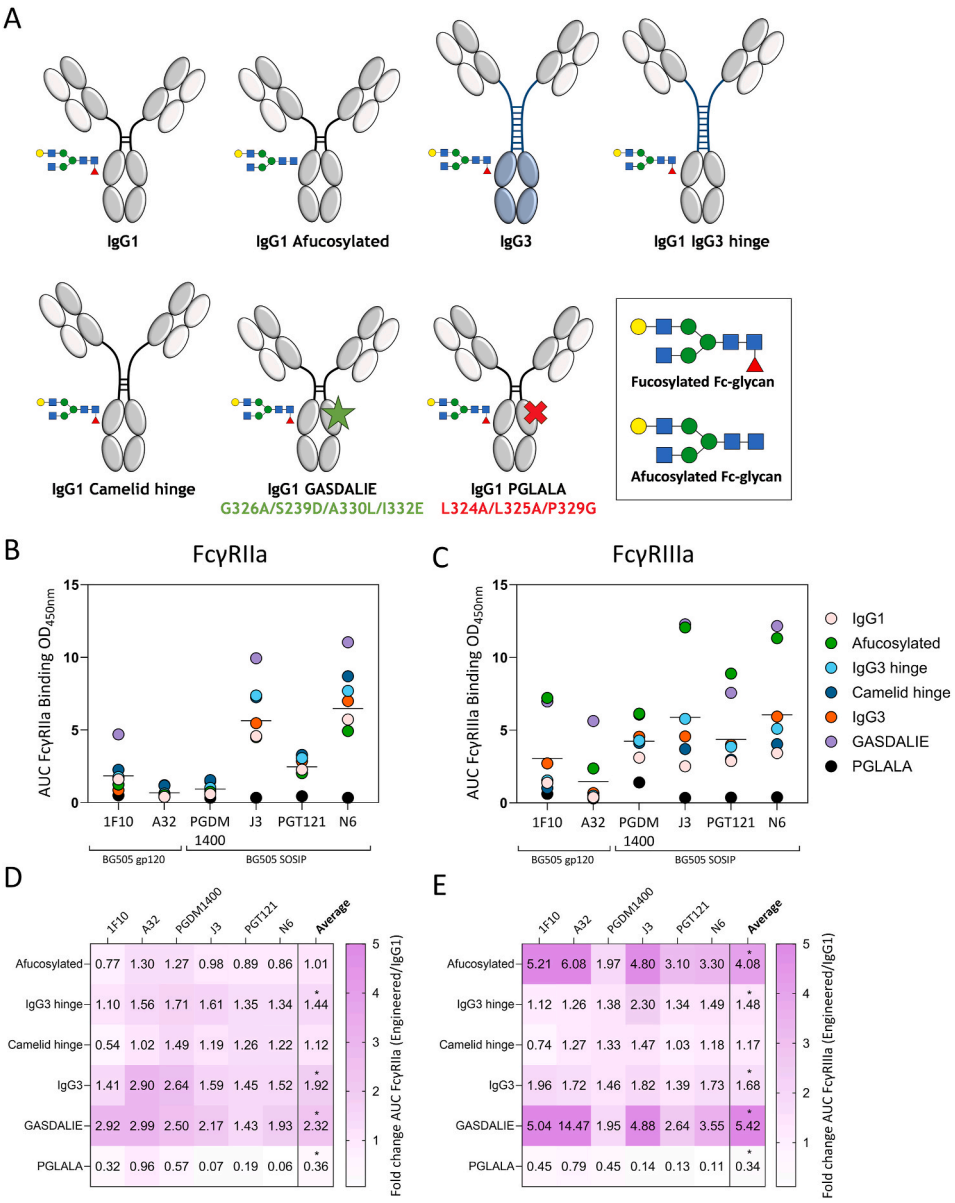

Fig. 1. Fc engineering results in enhanced FcγR binding. (A) Schematic visualization of the Fc engineered antibodies. The most abundant glycoform at position *N*297 is depicted on one of the heavy chains for each engineered antibody. Binding of anti-HIV-1 engineered antibodies to Fc receptors using BG505 SOSIP (PGDM1400, PGT121, N6, and J3) or BG505 gp120 (A32 and 1F10) as coating antigen. (B) Binding to FcγRIIa and (C) FcγRIIIa, plotted as area under the curve (AUC) values derived from an antibody titration from 5 to 0.001 μg/ml. Data are the representative of three independent experiments. (D) Heatmap illustrating the fold change in FcγRIIa binding (AUC) and (E) fold change in FcγRIIIa binding (AUC) of the engineered antibodies compared to their IgG1 counterparts. Wilcoxon matched pairs signed rank *t*-test were used to compare IgG1 and engineered antibodies with significance indicated as *p < 0.05.

increase in binding to FcγRIIa (1.44-fold and 1.92-fold respectively) and FcγRIIIa (1.48-fold and 1.68-fold respectively) compared to IgG1 antibodies. Afucosylated antibodies demonstrated a significant increase (4.1-fold) in binding to FcγRIIIa compared to IgG1 antibodies, with similar binding to FcγRIIa. Antibodies with a camelid hinge did not exhibit a significant increase in binding to FcγRIIa and FcγRIIIa. Finally, IgG1 variants bearing the PGLALA mutations were not binding to FcγRIIa or FcγRIIIa (Fig. 1B and C). The individual engineering strategies showed a uniform effect across the different anti-HIV-1 antibodies. The slight variation in the magnitude of the effect in different antibodies might be explained by the variation in opsonization and affinity. In conclusion, Fc engineering strategies can effectively enhance the affinity for FcγRIIa, FcγRIIIa, or both receptors, depending on the specific engineering strategy employed and without affecting HIV-1 Env binding.

2.2. Long hinge and IgG3 antibodies enhanced ADCP activity

Next, ADCP activity of engineered variants was evaluated by measuring the uptake of BG505 SOSIP.664 (PGDM1400, N6, PGT121, J3) or BG505 gp120 (A32 and 1F10) coated beads by THP-1 cells (Fig. 2A). Antibodies with an IgG3 hinge and full IgG3 backbone demonstrated significantly increased levels of ADCP (Fig. 2B–D). Interestingly, while the GASDALIE antibodies exhibited significantly enhanced binding to FcγRIIa, this resulted in only a slight and non-significant increase in ADCP (Fig. 2B). Conversely, antibodies with a camelid hinge did not display a notable improvement in FcγRIIa binding, yet they did enhance ADCP. As expected, the afucosylated antibodies induced similar levels of ADCP compared to the IgG1 antibodies (Fig. 2B). The absence of a significant difference between the IgG1 and PGLALA variants can be attributed to low FcγRIIa binding and potency

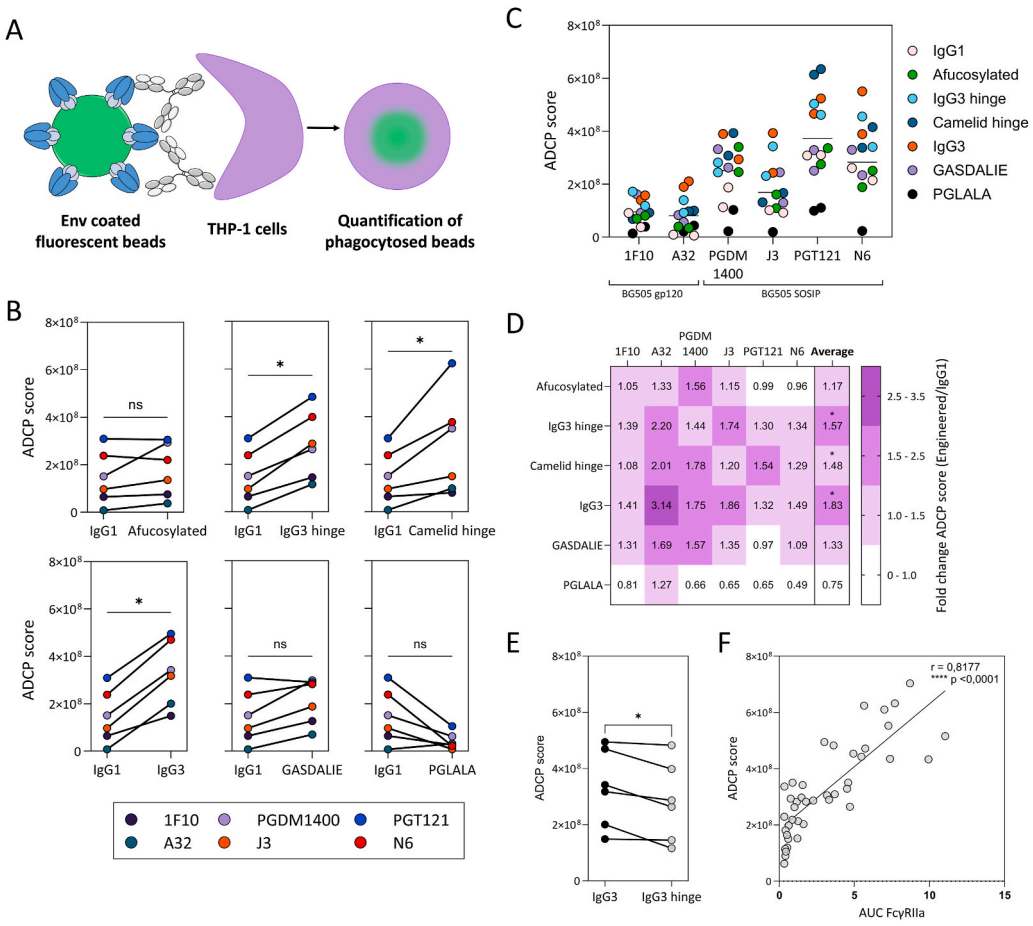

Fig. 2. Long hinge and IgG3 antibodies enhanced ADCP activity. (A) Visual representation of the ADCP assay. ADCP was measured by the fluorescent signal of THP-1 cells through the uptake of opsonized BG505 SOSIP.664 (PGDM1400, PGT121, N6, and J3) or BG505 gp120 (A32 and 1F10) coated fluorescent beads. (B) Change in ADCP score between IgG1 and engineered antibodies at a bNAb concentration of 100 nM. Each dot represents an individual anti-HIV-1 antibody. Statistical comparisons between IgG1 and engineered antibodies were performed using the Wilcoxon matched pairs signed-rank test, with significance indicated as *$p < 0.05$ or ns (non-significant). Data are representative of at least two independent experiments. (C) ADCP scores of the complete panel of antibody variants in two independent ADCP assays at a bNAb concentration of 100 nM. (D) Heatmap showing the fold change in ADCP scores of engineered antibodies relative to their IgG1 counterparts. (E) Change in ADCP score between IgG3 and IgG1 IgG3 hinge Abs at a bNAb concentration of 100 nM. Wilcoxon matched pairs signed rank *t*-test were used to compare IgG3 and engineered Abs with significance indicated as *$p < 0.05$. (F) Correlation plot between ADCP score and FcγRIIa binding using Spearman's correlations where **** denotes $p < 0.0001$.

of parental IgG1 antibodies, such as A32 (de Taeye et al., 2024) and PGDM1400 (Fig. 2C). Across the engineering strategies, full IgG3 antibodies showed the largest increase in ADCP score (average 1.83-fold) compared to IgG1 (Fig. 2D). IgG3 antibodies were found to induce significantly more ADCP compared to IgG1 antibodies with an IgG3 hinge, underscoring the critical role of the Fc-FcγR interaction (Fig. 2E). We observed a correlation between the binding to FcγRIIa and ADCP, indicating that FcγRIIa binding is predictive for the ability to induce ADCP ($r = 0.8177$, $p < 0.0001$) (Fig. 2F). Similar to the FcγRIIa binding ELISA, individual engineering strategies exhibited a consistent effect across the various anti-HIV-1 antibodies. Remarkably, the Fc engineering strategies employed in this study yielded similar effects in binding FcγRIIa and mediating ADCP in a nanobody-Fc construct (J3) and an IgG1*01 antibody (N6), both targeting the CD4bs. This observed uniformity in FcγRIIa-mediated phagocytosis suggests a degree of robustness in the engineering strategies across the antibody formats tested. Overall, these results show that subclass and hinge engineering strategies are most useful when aiming for increased ADCP of anti-HIV-1 antibodies.

2.3. Improved NK-cell activation by afucosylated and GASDALIE antibodies

Next, we investigated the effect of the engineering strategies on NK cell activation (IFNγ), degranulation (CD107) and receptor shedding (CD16) by stimulating primary NK cells with the various engineered anti-HIV-1 Abs in a plate-based assay (Fig. 3A) using His-tagged BG505 SOSIP.664 (PGDM1400, N6, PGT121, J3) or BG505 gp120 (A32, 1F10). The afucosylated antibodies, along with antibodies carrying the GASDALIE mutations, demonstrated the highest level of NK cell activation as measured by a significant increase in CD107+IFNγ+ double positive cells, and increased CD16 shedding (Fig. 3B). This resulted in an average fold change of CD107+IFNγ+ cells and CD16^{+} cells compared to IgG1 of 6.82 and 6.94, and 5.16 and 4.33, respectively (Fig. 3C). Despite a modest increase in FcγRIIIa binding, IgG3 antibodies did not show significantly enhanced NK cell activation. Additionally, both hinge elongation strategies had no significant effect on NK cell activation (Fig. 3C). Consistently, we observed relatively low signals for both A32 and PGDM1400 antibodies. The low signal for A32 antibodies, also noted in the ADCP assay, likely stems from relatively poor opsonization of gp120 and suboptimal orientation of the Fc domain (Fig. 3D). For PGDM1400, its differing stoichiometry (1:1) compared to other

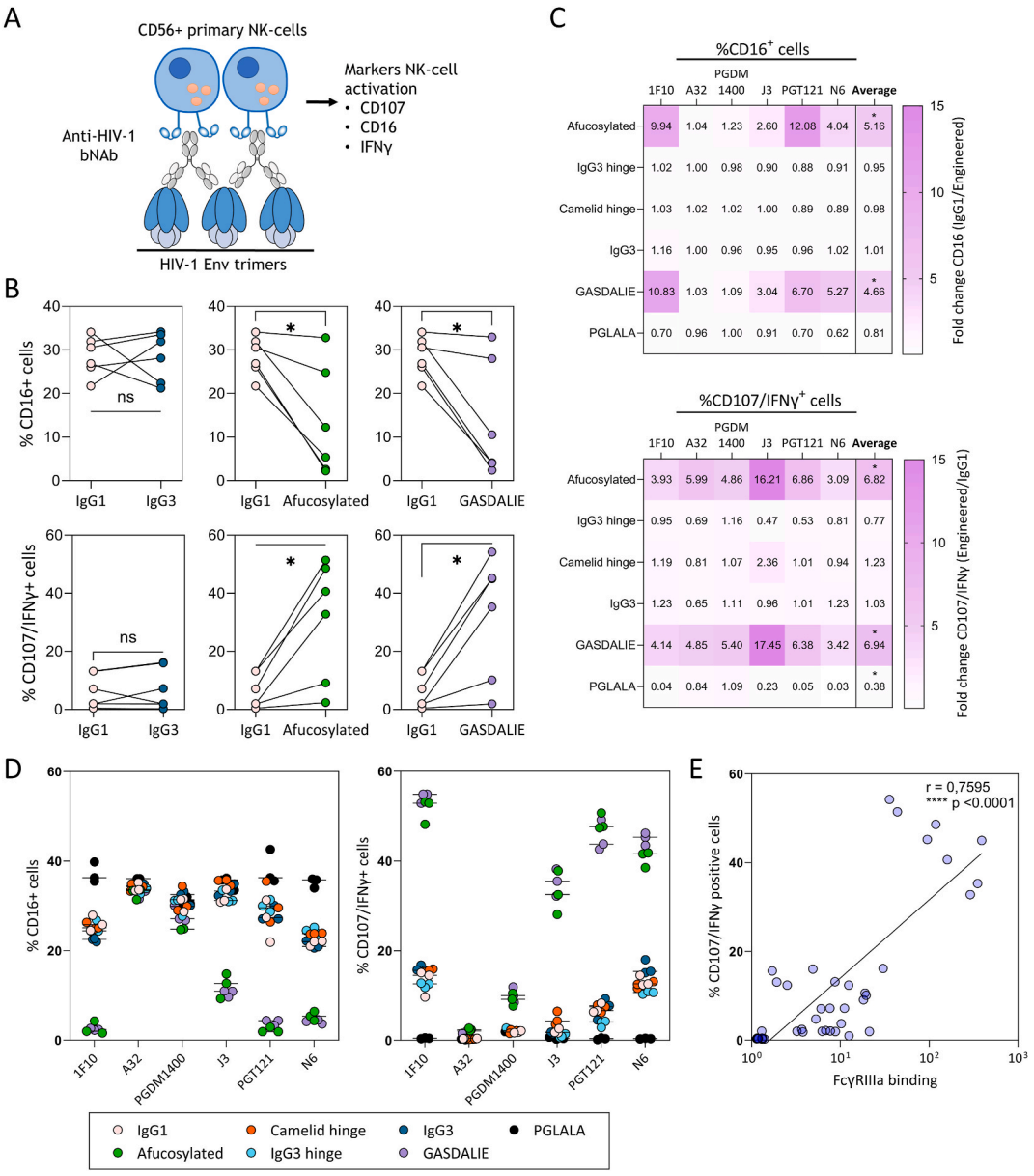

Fig. 3. Improved NK-cell activation by afucosylated and GASDALIE antibodies. (A) Visual representation of the plate-based NK activation assay. CD56$^+$ isolated NK-cells from buffy coats were incubated for 3 h with HIV-1 Env (BG505 SOSIP.664 for PGDM1400, PGT121, N6, and J3 and BG505 gp120 for A32 and 1F10) bound antibodies. Degranulation (CD107), activation (IFNγ) and CD16 shedding was analyzed with flow cytometry. (B) Change in %CD16+ and %CD107/IFNγ+ NK cells between IgG1 and engineered bNAbs at 100 nM. Each dot represents one of the anti-HIV-1 antibodies. Wilcoxon matched pairs signed rank *t*-test were used to compare IgG1 and engineered Abs with significance indicated as *$p < 0.05$, ns, non-significant. (C). Heatmaps showing the fold change in NK activation, measured by the change in CD16 (calculated as IgG1/Engineered) and IFNγ/CD107 (calculated as Engineered/IgG1) positive NK cells. (D) Percentage CD16$^+$ and CD107/IFNγ+ NK cells displayed for the six engineered anti-HIV-1 antibody sets. Data are the representative of three independent experiments. (E) Correlation plot between NK activation and FcγRIIIa binding using Spearman's correlations where **** denotes $p < 0.0001$.

antibodies (3:1) may contribute to reduced opsonization and, consequently, lower activation signals. The percentage of CD107+IFNγ+ double positive NK cells was correlated with FcγRIIIa binding ($r = 0.76$, $p < 0.0001$), indicating that FcγRIIIa binding is predictive of the ability to induce NK cell activation (Fig. 3E). Overall, the Fc engineering strategies employed in this study resulted in consistent outcomes in FcγRIIIa-mediated NK cell activation across two distinct antibody formats, highlighting the robustness of these strategies. In summary, these findings demonstrate that both glyco-engineering and Fc-engineering approaches can effectively enhance NK cell activation.

2.4. Combining engineering strategies

While we also found strategies that enhance ADCP activity, the engineering strategies focusing on FcγRIIIa binding and ADCC showed a more pronounced effect. We sought to further improve NK cell activation and ADCC activity by combining the glyco-engineering (afucosylation) and protein engineering (GASDALIE mutations) strategy. We produced double engineered PGT121, N6, J3 and 1F10 IgG1 antibodies, harboring the GASDALIE mutations in HEK293F cells in the presence of 2FF (Sup Fig. 5A). The double engineered antibodies retained similar neutralization compared to their IgG1 counterpart (Sup Fig. 3C). PGDM1400 and A32 antibodies were excluded from the analysis due to their low signal and potency observed in (previous) plate-based assays

(Sup Fig. 5B). Subsequently, we assessed the antibodies for their binding to human FcγRIIIa after binding BG505 SOSIP.664 (J3, N6, PGT121) or BG505 gp120 (1F10) (Fig. 4A). We observed that the antibodies that were both afucosylated and harboring GASDALIE mutations exhibited an almost 10-fold higher binding strength to FcγRIIIa compared to the WT IgG1 (Fig. 4B). In contrast, the single-engineered antibodies led to an average 7-fold increase in FcγRIIIa binding compared to WT IgG1. Furthermore, the double-engineered antibodies exhibited a 1.3-fold higher binding strength to FcγRIIIa compared to the single-engineered antibodies. It should be noted that while the difference between WT and afucosylated antibodies was statistically significant in Fig. 1E, this significance was not observed in Fig. 4B, likely due to a power issue arising from the use of only four antibody sets instead of six. Overall, these results suggest that the combination of N-glycan afucosylation and the GASDALIE mutations enhances FcγRIIIa binding. The enhanced effect of combining engineering strategies was also evident in the increased activation of NK cells by the double-engineered variant compared to the single-engineered variants (Fig. 4C). Even at lower concentrations (0.1 nM), increased NK cell activation remained visible, highlighting the potency of these antibodies. Across all the different anti-HIV-1 antibodies, the double-engineered variants induced the strongest NK cell activation, as evidenced by elevated CD107+IFNγ+ expression and increased CD16 shedding (Fig. 4D and E and Sup Fig. 5B). These findings demonstrate the potential of combining engineering strategies to achieve enhanced immune cell activation, which could aid in the killing of infected cells.

2.5. ADCC of HIV-1 infected cells by engineered Abs

We next assessed the ability of the engineered antibodies to induce specific activation of NK cells in a cellular context using the latently infected cell line ACH-2. PBMCs from HIV-1 negative donors were cocultured for 4h with ACH-2 cells in the presence of antibodies. Addition of afucosylated antibodies, GASDALIE antibodies, as well as the double-engineered variants, resulted in increased levels of IFNγ, CD107, along with decreased CD16 expression (Fig. 5A–C). While not reaching statistical significance, the double-engineered variants exhibited a slightly more effective activation of NK cells compared to the single-engineered variants. Within the ACH-2 cell population, we examined levels of p24 and cell viability. The use of IgG3 and longer hinge variants did not lead to a reduction in p24 levels. In contrast, antibodies that exhibited enhanced NK cell activation —afucosylated antibodies, GASDALIE antibodies, and the double-engineered variants —showed decreased p24 levels and increased cell death (Fig. 5D and Sup Fig. 6A and B). These two latter parameters showed a strong correlation ($r = 0.80$, $p < 0.0001$) (Sup Fig. 6C). Furthermore, we did not observe a correlation between antibody binding and ADCC activity (Sup Fig. 6D).

Next, we assessed the ability of the most potent N6 and PGDM1400 variants: the afucosylated, GASDALIE and double-engineered antibodies, to induce ADCC of a LAI-infected CEM-NKr-CCR5.luc cell line. ADCC capacity of the antibodies was measured by a loss of luciferase activity in the presence of antibody and healthy donor PBMCs. This revealed that afucosylated antibodies, antibodies harboring the GASDALIE mutations induced increased levels of ADCC compared to their IgG1 counterparts (Fig. 5E), and that the double-engineered variants exhibit an even higher capacity to mediate ADCC compared to the single-engineered antibodies. Notably, this improvement in ADCC activity of the single and double-engineered antibodies persists even at lower concentrations, underscoring the potency of engineered antibodies (Sup Fig. 7A). Further cellular analysis unveiled a decrease in p24+ cells for both the single and double-engineered antibodies, with the double-engineered variants displaying the highest efficacy (Fig. 5F), with almost no alteration in p24 levels by the IgG1 variant of both N6

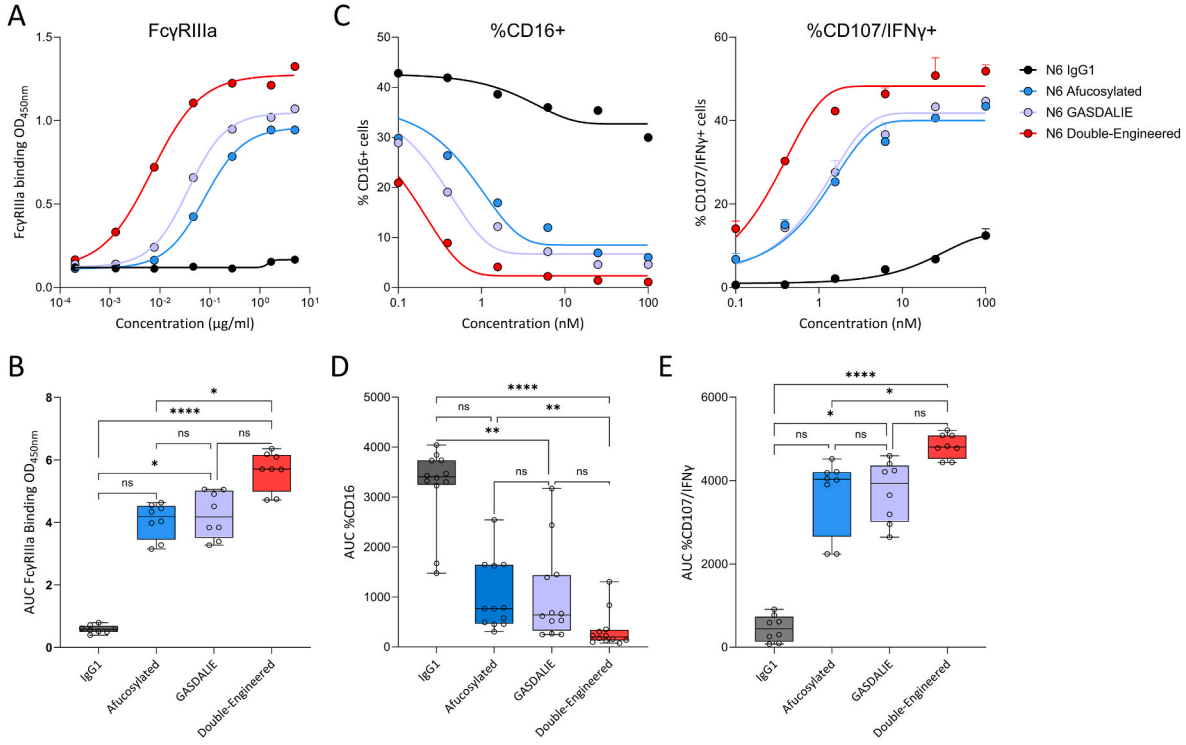

Fig. 4. Combination of engineering strategies results in enhanced FcγRIIIa binding and NK activation. (A) Binding of N6 engineered antibodies to FcγRIIIa as determined by FcγR dimer ELISA using BG505 SOSIP.664 as coating antigen. (B) Binding of J3, 1F10, PGT121 and N6 anti-HIV-1 antibodies to FcγRIIIa represented as AUC. Each dot represents the AUC value of replicates. (C) Curves illustrating the expression of NK cell activation markers, CD16 and CD107/IFNγ, in response to different N6-engineered antibodies. NK activation measured by (D) CD16 shedding and (E) degranulation (CD107), activation (IFNγ) of NK cells after incubation with J3, 1F10, PGT121 and N6 variants. NK activation markers represented as AUC. Each dot represents the AUC value of replicates. Statistical comparison between engineered antibody groups were performed using a Friedman test followed by a Dunn's multiple comparison (*$p < 0.05$, **$p < 0.01$, ****$p < 0.0001$).

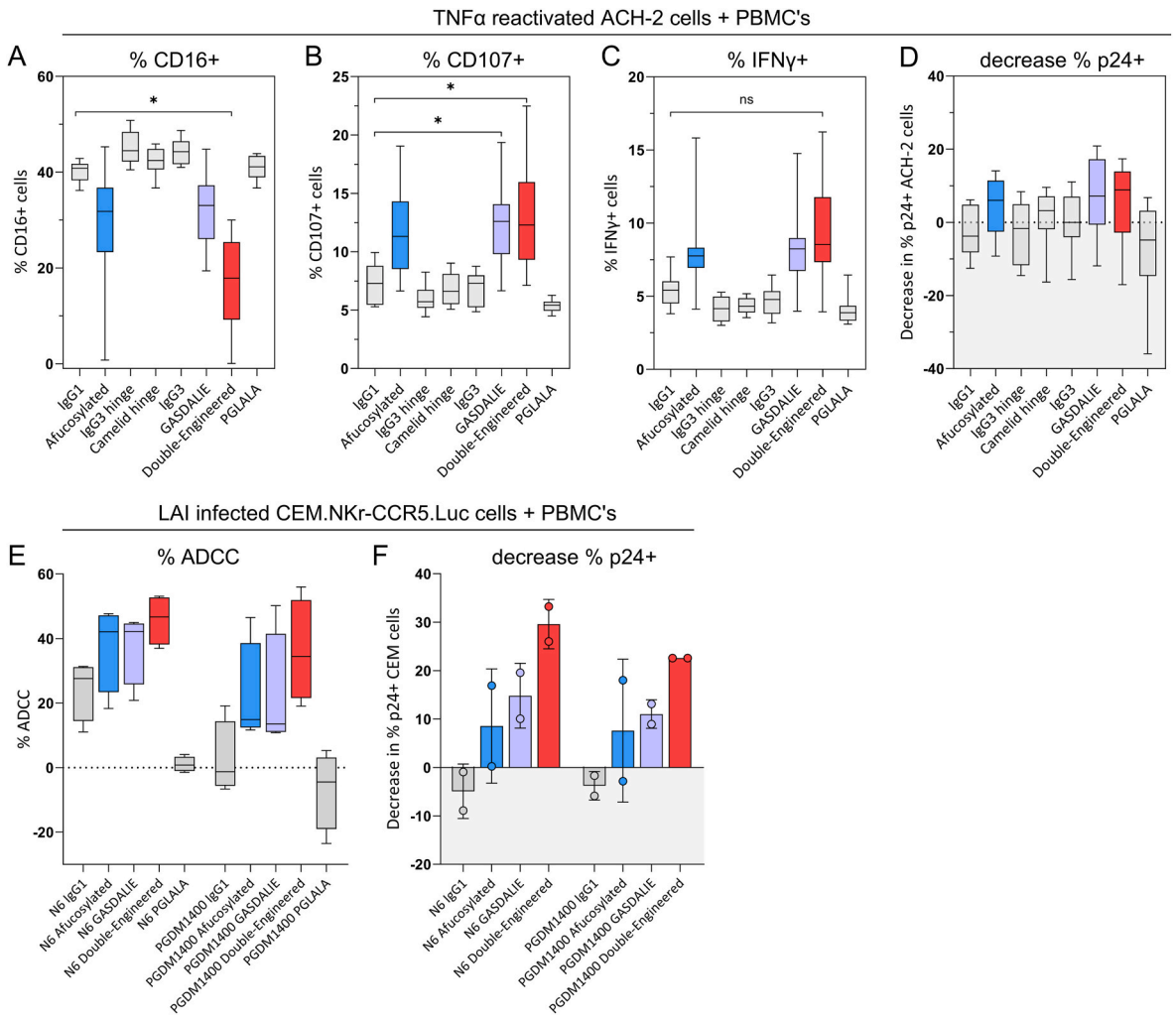

Fig. 5. Antibodies with enhanced FcγRIIIa binding induce killing of infected cells. Immune cell activation was assessed using the following parameters: (A) % CD16-positive cells (B) % CD107-positive cells (C) % IFNγ-positive $CD3^{-}CD19^{-}$ PBMCs upon incubation with engineered antibodies at 100 nM. (D) Decrease in the percentage of p24-positive ACH-2 cells compared to the no antibody control. Data is the representative of three independent experiments. (E) The percentage of ADCC was measured in CEM.CCR5.luc cells infected with the LAI strain, determined by a loss of luciferase activity in the presence of antibody and healthy donor PBMCs. The data includes results for both N6 and PGDM1400 antibodies at 50 nM. NK-cell mediated ADCC was measured using PBMCs from two individual donors, with combined data from both donors presented. (F) The decrease in the percentage of p24-positive LAI-infected CEM.CCR5.Luc cells compared to the no antibody control at a concentration of 50 nM. Statistical comparison between engineered antibody groups were performed using a Friedman test followed by a Dunn's multiple comparison (*$p < 0.05$).

and PGDM1400, highlighting the efficacy of engineering strategies in reducing the viral reservoir. Furthermore, we observed a correlation between the level of ADCC and the decrease in p24 level ($r = 0.7298$, $p < 0.0005$) (Sup Fig. 7B).

Overall, we show here that anti-HIV-1 antibodies with enhanced FcγRIIIa binding induce NK-cell mediated ADCC of latently infected cells, and have the potential to contribute to combinatorial HIV-1 cure strategies.

3. Discussion

Fc engineering in the field of HIV-1 has garnered increased interest, as it could lead to enhanced eradication of HIV-1 infected cells and contribute to durable control. In this study, we conducted a functional comparison of Fc engineering strategies using a panel of HIV-1 antibodies to assess their impact on Fc effector functions and their potential role for HIV-1 therapy.

Enhanced FcγRIIa binding and ADCP was achieved by IgG3 and longer hinge variants. IgG3 is an antibody subclass that naturally exhibits enhanced Fc-mediated effector functions compared to other IgG subclasses (Vidarsson et al., 2014). IgG3 has a longer hinge region, allowing for greater flexibility and increased accessibility to FcγRs on effector cells, which contributes to enhanced phagocytosis (Chu et al., 2020; Richardson et al., 2019). Interestingly, our study revealed that a longer hinge did not benefit NK activation. This aligns with previous studies showing that increasing the hinge length of anti-HIV-1 antibodies did not improve ADCC (Chu et al., 2020), whereas shortening the hinge did lead to increased ADCC, possibly due to altered proximity at the immunological synapse (De Taeye et al., 2020; Redpath et al., 1998). It has been suggested that while membrane-proximal epitopes are efficient for mediating effector functions like ADCC and CDC, epitopes positioned at an intermediate distance from the membrane facilitate optimal ADCP (Cleary et al., 2017). ADCP involves complex intracellular reorganization to form a phagocytic cup. Antibodies close to the membrane may face steric hindrance, hampering efficient phagocytosis. Conversely, epitopes more distal from the membrane allow better accessibility, facilitating stable multimeric complex formation and effective phagocytosis (Cleary et al., 2017; Van Erp et al., 2019; Bakalar et al., 2018; Freeman et al., 2016). A correlation between antibody binding and ADCC activity was previously found for a panel of

well-characterized bnAbs (Bruel et al., 2016). Apex-targeting bnAbs often show discrepancies between binding and ADCC activity, indicating that other factors such as antibody orientation and Fc topology also contribute to ADCC initiation (Bruel et al., 2016; Ren et al., 2020). Similarly, we found that PGDM1400 showed strong binding to reactivated ACH-2 cells, but failed to induce strong ADCC activity against these cells. Furthermore, our study suggests that the type of infected cell may influence epitope exposure, adding further complexity to ADCC activity. While PGDM1400 performed relatively poorly against reactivated ACH-2 cells (harboring the LAI strain), it was among the better-performing antibodies against LAI-infected CEM.NKR-CCR5-Luc cells. This underscores the complexity of epitope availability, which is influenced by the viral strain but may also be affected by the type of host cell.

A similar complexity was observed with A32, a non-neutralizing antibody selected for its ability to mediate ADCC (Ferrari et al., 2011; Tuyishime et al., 2020). Unlike other antibodies whose epitopes are readily accessible, the epitope of A32 (inner domain, cluster A region only becomes exposed after CD4 induced conformational changes of HIV-1 Env, which may limit its ADCC efficacy depending on the cell-type. To overcome this limitation, A32 is often paired with CD4 mimetics, which enhance its ADCC activity (Richard et al., 2021). While studies have shown that A32 can induce ADCC, the frequent shedding of gp120 and observed bystander killing, complicates the interpretation of A32's ADCC activity (Lewis et al., 2019; Richard et al., 2018). Thus, the potency of A32-mediated ADCC may vary across different viral strains, as the exposure of its target epitope on Env-infected cells differs significantly between viral isolates (Bruel et al., 2016).

Contrary to expectations, GASDALIE (G326A/S239D/A330L/I332E) antibodies exhibited increased FcγRIIa binding but only a slight improvement in ADCP. In contrast, a recent study found that other bNAbs carrying these mutations showed significantly enhanced phagocytic activity (Edwards et al., 2021). The GASDALIE mutations drive the interaction with FcγRIIb (Lazar et al., 2006) and while this receptor is only expressed at very low levels on THP-1 cells (Tridandapani et al., 2002; Robinson et al., 2018), enhanced binding by GASDALIE antibodies to this receptor could possibly inhibit potent activation of the cells. FcγRIIb is not expressed on NK cells (Nimmerjahn et al., 2006), explaining why this inhibition does not happen in the context of NK cell activation. However, the underlying explanation is likely to be more complex, implying that, in this context and assay, a flexible hinge could be more important for inducing ADCP than just strong binding to FcγRIIa. This holds true for PGT121, the only antibody where the GASDALIE mutations failed to enhance ADCP, yet where hinge elongation did lead to improvement. Furthermore, the discrepancy between antibodies with a camelid hinge and GASDALIE antibodies highlights the inadequacy of relying solely on FcγR binding assays to predict effector function. Despite less FcγRIIa binding, camelid hinge antibodies showed higher ADCP levels compared to GASDALIE antibodies. This emphasizes the necessity of functional assays in assessing antibody efficacy, as FcγR binding alone does not always correlate with effector function.

In this study, we demonstrated that improved FcγRIIIa binding, and NK-cell activation can be achieved through afucosylation and introducing GASDALIE mutations in anti-HIV-1 antibodies. Importantly, we showed that combining both engineering strategies results in enhanced FcγRIIIa binding and stronger NK cell mediated ADCC. This aligns with a study where an afucosylated antibody with S239D/S298A/I332E mutations notably increased NK cell activation compared to single engineered antibodies (Zhong et al., 2022). On the contrary, another study demonstrated that combining glyco-engineering with point mutations enhanced CD16a binding, but did not result in improved NK cell activation (Repp et al., 2011). These discrepancies may be attributed to the nature of the epitope, variations in the introduced mutations, and differences in the assay setup.

This study suggest that strategies aimed at enhancing NK-cell-mediated ADCC could be particularly relevant for the elimination of established viral reservoirs. This aligns with studies showing that NK cell responses contribute to HIV-1 immune control in ECs (Guo et al., 2022; Hartana et al., 2023). NK cells secrete cytokines and chemokines, affecting antiviral responses and reducing HIV-1 infectivity of target cells. Thus, enhancing the Fc:FcγRIIIa interaction stands out as a promising strategy for HIV-1 cure approaches (Duan et al., 2022; Alrubayyi et al., 2022). In contrast, strategies aimed at enhancing ADCP, such as using IgG3 antibodies in the presence of full PBMCs (which include monocytes and macrophages capable of mediating ADCP), did not lead to a reduction in p24 levels in either infected CEM cells or reactivated ACH-2 cells. While IgG3 antibodies may facilitate the phagocytic clearance of virally infected cells, they may not be as effective in engaging immune cells for the same level of killing seen with ADCC-focused strategies. Strategies aimed at enhancing ADCP would be more beneficial for bNAbs administered at the time of ART or during ATI, improving uptake and crosstalk between antigen presenting cells and T cells. More research is necessary to investigate how ADCP-promoting antibodies, such as IgG3, can contribute to reaching durable control and if antibody engineering can contribute to the vaccinal effect (Naranjo-Gomez et al., 2023). Recently, a bNAb with S239D/A330L/I332E (SDALIE) mutations was administered during the acute phase of SHIV infection in non-human primates, resulting in significantly higher levels of activated CD8 T cells compared to the wild-type antibody (Dias et al., 2024). While it remains unclear whether this effect was mediated through FcγRII or FcγRIII functions, it underscores the potential benefits of developing bnAbs with enhanced affinity to FcγRs for HIV-1 therapy.

It is noteworthy that Fc engineering strategies used in this study had similar effects in a nanobody-Fc construct and an IgG1*01 antibody both targeting the CD4bs. This suggests that these engineering strategies may have broader applicability across various antibody formats, potentially expanding their use in therapeutic antibody development.

To advance this study, additional information is essential regarding the potency and immunogenicity of the antibodies. In terms of potency, it is crucial to determine if the constructs can effectively eliminate infected cells while preventing the infection of uninfected cells. Moreover, valuable insights can be gained from the use of primary cells from PWH, who typically exhibit a more immunocompromised profile, such as whether the route of activation is not limited by the downregulation of activating receptors (Duan et al., 2022; Mikulak et al., 2017; Pace et al., 2022). Additionally, exploring the potential synergies between antibody therapies and latency reversal agents (LRAs) to target latent HIV reservoirs holds substantial promise. Combinations with multiple LRAs may effectively reduce the viral reservoir, thereby augmenting the efficacy of antibody-based therapies in achieving an HIV-1 cure (Tuyishime et al., 2020; Davis-Gardner et al., 2017).

Overall, this study provides valuable information in antibody engineering, presenting potential approaches to strengthen immune responses, especially through activation of NK cells. Further studies on enhancing antibody potency and exploring engineering combinations could yield more effective antibody-based HIV-1 treatments and potential HIV-1 cure strategies.

4. Methods

4.1. Cells

The Laboratory for Viral Immune Pathogenesis at the AMC gifted the THP-1 cells, which were cultured at 37 °C, 5% CO_2 in RPMI 1640 Medium (ThermoFisher) with 10% fetal calf serum (FCS, Gibco) and 1/1000 Penicillin Streptomycin (P/S, Gibco). To maintain a density of 0.5–1 × 10^6 cells/mL, cells were passaged three times a week. The AIDS Reagent Program provided TZM-bl cells, a HeLa cell line, which were cultured at 37 °C, 5% CO_2 in DMEM (ThermoFisher) with 10% FCS and 1/1000 P/S. Cells were passaged twice a week to maintain a confluency

of 10–90%. HEK-293F cells (Invitrogen) were cultured at 37 °C, 5% CO_2 in Freestyle medium (Life Technologies) at a density of 1 × 10^6 cells/mL. To maintain a density of 0.5–1 × 10^6 cells/mL, cells were passaged three times a week. The Laboratory for Viral Immune Pathogenesis at the AMC gifted the ACH-2 cells, a latently cell line infected with HIV-1 isolate LAI, which were cultured at 37 °C, 5% CO_2 in IMDM Medium (ThermoFisher) with 10% fetal calf serum (FCS, Gibco) and 1/1000 Penicillin Streptomycin (P/S, Gibco). To maintain a density of 0.5–1 × 10^6 cells/mL, cells were passaged two-three times a week. CEM.NKR-CCR5-Luc (AIDS Reagent Program) were cultured at 37 °C, 5% CO2 in IMDM Medium (ThermoFisher) with 10% fetal calf serum (FCS, Gibco) and 1/1000 Penicillin Streptomycin (P/S, Gibco) and split twice a week to maintain a density of 0.5–1.5 × 10^6 cells/mL.

4.2. Cloning

G-blocks were ordered for the IgG3 Fc, IgG3 hinge and camelid hinge, for both the IgG1*01 and nanobody constructs. These DNA fragments (Integrated DNA Technologies, Inc) were designed with overhangs to facilitate cloning into the AbVec-HigG plasmid using the Gibson assembly technique. Gibson mix was incubated with the vector and insert DNA for 1 h at 50 °C. After incubation, XL-1 blue cells were added to the Gibson mix, incubated on ice for 30 min before heat-shock activation (45 s, 42 °C). The bacteria/plasmid mix was further incubated for 1 h at 37 °C with 2x Lysogeny broth (LB). The bacteria mixture was plated out on 2xLB plates containing 100 mg/ml ampicillin and incubated overnight at 37 °C. After incubation, colonies were picked, grown, and purified using the plasmid DNA purification kit (Macherey-Nagel). The DNA was sequenced by Macrogen Europe B.V using Sanger sequencing and correct clones were selected for further use. Using Q5 Site-Directed mutagenesis (BioLabs) the mutations: G236A, S239D or L234A, L235A, P329G were incorporated into the antibody plasmid. Primers were designed using the NEBaseChanger tool (Biolabs). Q5 Hot Start High-Fidelity 1x master mix, 10 μM forward primer, 10 μM reverse primers and the template DNA (1–25 ng/μl) were mixed and exponentially amplified using PCR (25 cycles), replicating the plasmid DNA with the mutation. Subsequently the DNA was incubated with a mixture of Kinase, Ligase & *Dpn*I (5 min RT) to allow phosphorylation, ligation, and the degradation of template DNA. Quickchange site-directed mutagenesis kit (New England Biolabs) was used to introduce the A330L and I332E mutations in the heavy chain plasmids. Primers were designed using the PrimerX tool (bioinformatics). The PCR reaction mixture contained 25 ng plasmid DNA, 10 μM forward primer, 10 μM reverse primer, 1x reaction buffer, dNTPs and 2.5 U/μl PfuTurbo DNA polymerase. After the PCR amplification, *Dpn*I restriction enzyme was added (10 U/μl) to the PCR reaction mixture and incubated at 37 °C for 1 h. After Q5 and Quickchange site-directed mutagenesis, transformation of XL-1 blue cells, and validation of correct clones was done as described previously. Amino acid sequences of the engineered antibody constructs can be found in (Sup Fig. 1).

4.3. Antibody production and purification

HEK-293F cells (1x10^6 cells/mL) were used for transient expression of the antibody constructs. At day 1, cells were transfected with the antibody plasmid and 1 μg/μl PEImax (Polysciences) in a 3:1 ratio in OptiMEM. For the production of afucosylated antibodies, 0.15 mM 2-deoxy-2-fluorofucose (2FF) (Carbosynth, MD06089) was added 1 h before transfection to the cells. The cells were harvested on day 6, and the supernatant was collected, followed by centrifugation (30 min, 4000 rpm) and filtration using 0.22 μm Steritop filters (Merck Millipore). Antibodies were purified using protein A/G (Pierce) affinity chromatography. Antibodies were eluted from the column using 0.1 M glycine (pH 2.5) and neutralized using neutralization buffer 1M Tris (pH 8.7). The eluates were concentrated, and buffer exchanged to PBS using 50 or 100 kDa Vivaspin filters (GE Healthcare) for Nanobody-Fc or IgG molecules, respectively.

4.4. IgG glycosylation analysis by mass spectrometry

Immunoglobulin G Fc N-glycosylation was analyzed through liquid chromatography – mass spectrometry, following previously published methods (Falck et al., 2017). 5 μg monoclonal antibody was mixed with 100 μL of 100 mM formic acid, incubated for 15 min, and then dried. The denatured antibodies were reconstituted in 50 mM ammonium bicarbonate, shaken for 5 min, and cleaved by adding 200 ng sequencing grade trypsin (Promega, Leiden, The Netherlands) at 37 °C overnight. The resulting glycopeptides were measured by injecting the sample onto a trap column, followed by reversed-phase separation on a nanoEase M/Z Peptide BEH C18 analytical column (75 μm × 100 mm, particle size 1.7 μm, poresize 130 Å, 1/PK, Waters) at a flow rate of 600 nL/min. Positive-mode electrospray ionization mass spectrometry (MS) was employed for detection. The instrumental setup utilized an Ultimate 3000 RSLCnano system (Dionex/Thermo Fisher Scientific, Sunnyvale, CA) and an Impact HD quadrupole-time-of-flight (qTOF)-MS (Bruker Daltonics, Bremen, Germany). A linear gradient of solvent A (0.02% TFA in water) and solvent B (95% CAN) was applied, with the following gradient profile: 3% B at 0 min, 21% B at 4.5 min, 50% B at 5.5 min, 50% B at 8 min, 3% B at 9 min, and 3% B at 11.5 min. Spectra were recorded at a frequency of 1 Hz within the m/z range of 550–1800. Data processing was conducted using LaCyTools version 2.0.1 build 20201216, following established parameters: no alignment; calibration and extraction mass window of 0.2 Da and 0.1 Th, respectively; and an extraction time window of 10.0 s.

4.5. SDS page

The antibodies were analyzed using SDS-PAGE followed by Coomassie blue dye staining. A total of 5 μg protein was mixed with loading dye (0.125 M Tris-HCl pH 6.8, 20% glycerol, 4% SDS, 0.05% bromephenol blue in Milli-Q water) and dithiothreitol (DTT; 50 mM). This mixture was incubated at 95 °C for 10 min before being loaded onto a 4–12% Tris-Glycine gel (Invitrogen). As a reference marker, Precision Plus Protein Standard Dual Color (Biorad cat#161–0374) was used. The gel was run for 2 h at 125V in running buffer (25 mM Tris, 192 mM glycine, 0.05% SDS). Following electrophoresis, the gel was stained using the PageBlue Protein Staining Solution (Thermo Scientific) for 60 min. Subsequently, the gel was destained using ultrapure water with gentle agitation.

4.6. Binding ELISA

Galanthus nivalis lectin (Vector Laboratories) was coated onto ELISA plates overnight at 4 °C in 0.1 M $NaHCO_3$. Following three washes with 1X Tris-buffered saline (TBS), residual binding was blocked with 50 μl of 1% (w/v) casein in TBS (Thermofisher) for 30 min at RT. Recombinant SOSIP.v9.0 trimers (2 μg/ml) were then added to the plates in casein in TBS, and incubated for 2 h at RT. For ELISAs using BG505 gp120 as a target, the same protocol was used. However, BG505 gp120 was directly coated onto ELISA plates overnight at 4 °C in PBS, and for all dilution steps 1xTBS supplemented with 2% milk was used. The plates were subsequently washed using TBS and incubated with serially diluted primary antibodies for 2 h at RT. After primary antibody incubation, the plates were incubated with horseradish peroxidase labeled secondary antibodies (goat anti-human IgG 1:3000) in 1% Casein in TBS for 1 h at RT. The plates were washed 5 times with 1X TBS/0.05% Tween-20, and the development solution (0.1 M sodium acetate + 0.1 M citric acid + 1% TMB + 0.01% H_2O_2) was added. The reaction was stopped after 2 min using 0.8 M H_2SO_4. The optical density was measured at 450 nm using a SPECTROstar Nano Microplate Reader (BMG LabTech).

4.7. FcγR dimer ELISA

For the assessment of FcγR binding, different proteins were employed for the different antibody sets. Specifically, plates were coated with BG505 gp120 for A32 and 1F10 antibodies. For J3, N6, and PGT121 antibodies, BG505 SOSIP.v9.0 was employed, while for PGDM1400 antibodies, His-tagged BG505 SOSIP was coated onto Ni-NTA plates (Qiagen). Galanthus nivalis lectin (Vector Laboratories) was coated onto ELISA plates overnight at 4 °C in 0.1 M NaHCO3. The plates were then washed three times with 1X TBS. Next, BG505 SOSIP.v9.0 trimer (2 μg/ml) in 1X DPBS was added to the plates and incubated for 2 h at 37 °C. BG505 gp120 and His-tagged BG505 SOSIP.v9.0, were coated directly (2 μg/ml) onto the plates overnight at 4 °C in PBS. The plates were washed four times with TBS-0.05% Tween-20 (TBS-T) and blocked with assay buffer (1% bovine serum albumin (BSA), 0.05% Tween-20, 1 mM EDTA in PBS) for 1 h at 37 °C. After blocking, the plates were washed four times with TBS-T and incubated with serially diluted primary antibodies (concentration range of 5 - 0.001 μg/ml) for 2 h at 37 °C. Biotinylated FcγRIIIa or FcγRIIa dimers (0.5 μg/ml), which were produced as described previously (Wines et al., 2016) in HEK-293F cells using PEImax, purified using NiNTA columns (Qiagen), and biotinylated using the Biotin-protein ligase kit (Sigma-Aldrich), were added to the plates and incubated for 1 h at 37 °C. The plates were washed and incubated with high sensitivity streptavidin-HRP detection antibody (1:2,000) in assay buffer for 1 h at 37 °C. Following incubation, the plates were washed four times with TBS-T. The development solution (0.1 M sodium acetate + 0.1 M citric acid + 1% TMB + 0.01% H_2O_2) was added and the reaction was stopped using 0.8 M H_2SO_4. The optical density was measured at 450 nm using a SPECTROstar Nano Microplate Reader (BMG LabTech).

4.8. Neutralization assay

Neutralization assays were performed as previously described (Schriek et al., 2022). Briefly, TZM-bl cells were seeded in DMEM supplemented with 10% FCS and 1/1000 P/S to achieve a confluency of 70–80%. The virus mix was then incubated with the antibodies for 1 h at room temperature to allow binding. Dextran (DEAE) and Saquinavir (SQV) were added to the cells at final concentrations of 40 μg/ml and 400 nM, respectively. Following this, the virus-antibody mixture was added to the cells and incubated at 37 °C for 72 h. After incubation, the cells were lysed with 1x lysis buffer and placed on an orbital shaker for 20 min at room temperature. Subsequently, 5 μl of the lysate and 25 μl of Bright Glo Luciferase reagent were added to a white 96-well plate, and luciferase activity was measured using a Glomax plate reader. The inhibitory concentration (IC50) was calculated as the concentration of mAb required to neutralize 50% of the virus, determined using a dose-response non-linear regression fit in GraphPad Prism 9.

4.9. Antibody-dependent cellular phagocytosis (ADCP)

Fluorescent Neutravidin beads (Invitrogen) were incubated with biotinylated BG505 SOSIP.664 or biotinylated BG505 gp120 (5 μg/10 μl beads) overnight at 4 °C. The unbound antigen was removed by washing the beads twice in PBS containing 2% BSA, which blocked the remaining hydrophobic sites on the microspheres. The coated beads were diluted 1:500 in PBS 2% BSA and 50 μl of the suspension was placed in each well of a V-bottom 96-well plate. After incubation with serially diluted antibodies at 37 °C for 2 h, 5×10^4 THP-1 effector cells (ATCC) were added to each well in a final volume of 100 μl. The plates were quickly spun down to promote beads to cell contact and incubated for 5 h at 37 °C. After incubation, the cells were washed and stained using a fixable viability dye ef780 (Biolegend). Afterwards, the cells were resuspended in PBS 2% FCS, and analyzed by flow cytometry to determine phagocytic activity. The phagocytosis was quantified using the ADCP score, defined as (beads-positive cells × mean FITC MFI) − MFI of the no-antibody control.

4.10. NK-activation assay

Peripheral blood mononuclear cells (PMBCs) were extracted from buffy coats (Sanquin) via Ficoll-Paque (Cytiva) following the manufacturer's instructions. NK cells were isolated through positive selection using microbeads against CD56 (Macs Miltenyi, Biotec). The eluted cells were suspended in PBS, pH 7.2, 0.5% (m/v) BSA, and 2 mM EDTA. The isolated NK cells were resuspended in IMDM (Thermofisher) with 10% fetal calf serum (FCS, Gibco), stimulated with IL-15 overnight (10 ng/ml, 37 °C) to prepare for use as effector cells. Ni-NTA plates or half-area plates were coated overnight at 4 °C with His-tagged BG505 SOSIP.664 or untagged gp120, respectively. Next day, plates were blocked with PBS-1% BSA for 1 h at 37 °C, followed by three washing steps with TBS. Serial dilutions of antibodies in PBS-1% BSA were added to the plates and incubated for 1 h at 37 °C, followed by another round of washing with TBS. Next, IL-15 stimulated NK cells (50,000 cells/well) with 1:1000 Brefeldin-A (Biolegend) were added and incubated for 3 h at 37 °C. The NK cells were transferred to a 96-well V-bottom plate, washed using FACS buffer (2% FCS, PBS), and stained with anti-CD16-PE (Biolegend), fixable viability dye ef780 (Biolegend) and anti-CD107a-APC (Biolegend) for 30 min at 4 °C. Next, cells were washed and fixated using Cytofix/Cytoperm Fixation/Permeabilization Kit (BDBiosciences) according to the manufactures protocol. Subsequently, cells were stained for IFNγ-PE (Biolegend) intracellularly for 30 min at 4 °C. Lastly, cells were washed and resuspended in PBS 2% FCS. Flow cytometry was used to determine the percentage of IFNγ/CD107 and CD16 positive cells in the live cell gate.

4.11. ACH-2 killing assay

$1x10^6$ ACH2 cells/mL in IMDM were stimulated overnight at 37 °C with 0.1 ng/mL TNFα. The next day, ACH2 cells were washed and stained using violet CellTrace (Invitrogen) (0.25 μM) for 20 min at 37 °C. Next, IMDM was added, and cells were incubated for 5 min at RT. The cells were spun down at 1100 rpm for 5 min and resuspended in culture medium. After a 10-min incubation, the cells were washed twice with IMDM. Next, 20,000 ACH2 cells were added to V-bottom 96-well plates and incubated with antibodies for 15 min at room temperature (RT). Afterwards, 180,000 PBMCs were added, and the plates were quickly spun down before incubation for 4 h at 37 °C. After incubation, plates were washed twice with PBS 2% FCS and stained with anti-CD16-PE (Biolegend), CD3 APC-eF780 (Invitrogen), CD19 APC-eF780 (Invitrogen), fixable viability dye ef780 (Biolegend), and anti-CD107a-APC (Biolegend) for 30 min at 4 °C. Next, cells were washed and fixated using Cytofix/Cytoperm Fixation/Permeabilization Kit (BDBiosciences) according to the manufactures protocol. Subsequently, cells were stained for anti-P24 FITC antibody (KC57) and IFNγ-PE (Biolegend) intracellularly for 30 min at 4 °C. Lastly, cells were washed and resuspended in PBS 2% FCS. Flow cytometry was used to analyze the cells, and the percentage of CD107, IFNγ, CD16 and p24 positive cells were determined.

4.12. ADCC assay

For the infection, CEM.CCR5.luc cells were washed once and resuspended in IMDM medium (containing penicillin/streptomycin and 10% FCS) at a concentration of 0.8e6 cells/ml. The cells were plated in 6-well plates (2 mL/well) and supplemented with 5 μg/ml DEAE. Subsequently, 20 μl of LAI virus stock was added to each well, and the plates were incubated at 37 °C for 2 h. Following the incubation, individual wells were washed in Eppendorf tubes and resuspended in IMDM +5 μg/ml DEAE. The plates were then incubated at 37 °C, and infection was monitored by observing syncytia formation and measuring luciferase activity in CEM.CCR5.luc cells on day 3 and day 4. On the day of the

experiment, 20,000 CEM.CCR5.luc cells were added to each well of a V-bottom 96-well plate with antibody dilutions, and binding was allowed for 15 min (RT). Afterwards, 50 μl of PBMCs (180,000 cells) were added. The plates were briefly spun down before a 6-h incubation at 37 °C. After incubation, half of the cells were lysed using 1x lysis buffer and incubated on an orbital shaker for 20 min at RT. Afterwards, 5 μl lysate and 25 μl Bright Glo Luciferase was added to a white 96 well plate and subsequently luciferase activity of cell lysate was measured using a Glomax plate reader. The rest of the cells were washed twice with PBS 2% FCS and stained with fixable viability dye ef780 (Biolegend) for 30 min at 4 °C. Next, cells were washed and fixated using Cytofix/Cytoperm Fixation/Permeabilization Kit (BDBiosciences) according to the manufactures protocol. Subsequently, cells were stained for anti-P24 FITC antibody (KC57) intracellularly for 30 min at 4 °C. Lastly, cells were washed and resuspended in PBS 2% FCS. Flow cytometry was used to analyze the percentage of p24 positive cells.

Funding

This work was supported by the Aidsfonds under grant number P-53301; amfAR Mathilde Krim fellowship under grant number 110425-73-RKRL; HealthHolland/Aidsfonds under grant number LSHM19101/P-44802; and HealthHolland/AMC under grant number 2019-1167. The first two grants are received by Steven de Taeye (SdT).

Disclosure of interest

The authors report no conflict of interest.

CRediT authorship contribution statement

Angela I. Schriek: Writing – review & editing, Writing – original draft, Visualization, Methodology, Investigation, Formal analysis, Data curation, Conceptualization. **David Falck:** Writing – review & editing, Formal analysis, Data curation. **Manfred Wuhrer:** Writing – review & editing, Formal analysis, Data curation. **Neeltje A. Kootstra:** Writing – review & editing, Supervision, Resources, Funding acquisition. **Marit J. van Gils:** Writing – review & editing, Supervision, Resources, Funding acquisition, Conceptualization. **Steven W. de Taeye:** Writing – review & editing, Supervision, Resources, Investigation, Funding acquisition, Conceptualization.

Declaration of competing interest

The authors declare that they have no known competing financial interests or personal relationships that could have appeared to influence the work reported in this paper.

Data availability

Data will be made available on request.

Acknowledgements

We thank Jan Nouta and Steinar Gijze for technical support of the IgG glycosylation analysis.

Appendix A. Supplementary data

Supplementary data to this article can be found online at https://doi.org/10.1016/j.antiviral.2024.106015.

References

Ahmed, A.A., et al., 2016. Structural characterization of GASDALIE Fc bound to the activating Fc receptor FcγRIIIa. J. Struct. Biol. 194 (1), 78–89.
Alrubayyi, A., Rowland-Jones, S., Peppa, D., 2022. Natural killer cells during acute HIV-1 infection: clues for HIV-1 prevention and therapy. AIDS 36 (14), 1903–1915.
Amitai, A., Chakraborty, A.K., Kardar, M., 2018. The low spike density of HIV may have evolved because of the effects of T helper cell depletion on affinity maturation. PLoS Comput. Biol. 14 (8), e1006408.
Bakalar, M.H., et al., 2018. Size-dependent segregation controls macrophage phagocytosis of antibody-opsonized targets. Cell 174 (1), 131–142. e13.
Barouch, D.H., et al., 2013. Protective efficacy of a global HIV-1 mosaic vaccine against heterologous SHIV challenges in rhesus monkeys. Cell 155 (3), 531–539.
Borducchi, E.N., et al., 2018. Antibody and TLR7 agonist delay viral rebound in SHIV-infected monkeys. Nature 563 (7731), 360–364.
Bruel, T., et al., 2016. Elimination of HIV-1-infected cells by broadly neutralizing antibodies. Nat. Commun. 7 (1), 1–12.
Busman-Sahay, K., et al., 2021. Eliminating HIV reservoirs for a cure: the issue is in the tissue. Curr. Opin. HIV AIDS 16 (4), 200.
Caskey, M., 2020. Broadly-neutralizing antibodies (bNAbs) for the treatment and prevention of HIV infection. Curr. Opin. HIV AIDS 15 (1), 49.
Chu, T.H., et al., 2020. Hinge length contributes to the phagocytic activity of HIV-specific IgG1 and IgG3 antibodies. PLoS Pathog. 16 (2), e1008083.
Cleary, K.L., et al., 2017. Antibody distance from the cell membrane regulates antibody effector mechanisms. J. Immunol. 198 (10), 3999–4011.
D'Eall, C., et al., 2019. Modulating antibody-dependent cellular cytotoxicity of epidermal growth factor receptor-specific heavy-chain antibodies through hinge engineering. Immunol. Cell Biol. 97 (6), 526–537.
Damelang, T., et al., 2024. Impact of structural modifications of IgG antibodies on effector functions. Front. Immunol. 14, 1304365.
Davis-Gardner, M.E., et al., 2017. eCD4-Ig promotes ADCC activity of sera from HIV-1-infected patients. PLoS Pathog. 13 (12), e1006786.
Dias, J., et al., 2024. Administration of anti-HIV-1 broadly neutralizing monoclonal antibodies with increased affinity to Fcγ receptors during acute SHIVAD8-EO infection. Nat. Commun. 15 (1), 7461.
Duan, S., Liu, S., 2022. Targeting NK cells for HIV-1 treatment and reservoir clearance. Front. Immunol. 13.
Edwards, J.M., et al., 2021. Enhancement of antibody-dependent cellular cytotoxicity and phagocytosis in anti-HIV-1 bovine chimeric broadly-neutralizing antibodies. J. Virol. JVI. 00219-21.
Van Erp, E.A., et al., 2019. Fc-mediated antibody effector functions during respiratory syncytial virus infection and disease. Front. Immunol. 10, 548.
Etemad, B., et al., 2023. HIV post-treatment controllers have distinct immunological and virological features. Proc. Natl. Acad. Sci. USA 120 (11), e2218960120.
Falck, D., et al., 2017. High-throughput analysis of IgG Fc glycopeptides by LC-MS. High-throughput glycomics and glycoproteomics. Methods and Protocols 31–47.
Ferrara, C., et al., 2011. Unique carbohydrate–carbohydrate interactions are required for high affinity binding between FcγRIII and antibodies lacking core fucose. Proc. Natl. Acad. Sci. USA 108 (31), 12669–12674.
Ferrari, G., et al., 2011. An HIV-1 gp120 envelope human monoclonal antibody that recognizes a C1 conformational epitope mediates potent antibody-dependent cellular cytotoxicity (ADCC) activity and defines a common ADCC epitope in human HIV-1 serum. J. Virol. 85 (14), 7029–7036.
Flerin, N.C., et al., 2019. Establishment of a novel humanized mouse model to investigate in vivo activation and depletion of patient-derived HIV latent reservoirs. J. Virol. 93 (6).
Flórez-Álvarez, L., Hernandez, J.C., Zapata, W., 2018. NK cells in HIV-1 infection: from basic science to vaccine strategies. Front. Immunol. 9, 409736.
Foss, S., et al., 2022. IgG3 hinge dependent enhancement of intracellular antiviral immunity. Science immunology 7 (70), eabj1640.
Freeman, S.A., et al., 2016. Integrins form an expanding diffusional barrier that coordinates phagocytosis. Cell 164 (1), 128–140.
Freund, N.T., et al., 2017. Coexistence of potent HIV-1 broadly neutralizing antibodies and antibody-sensitive viruses in a viremic controller. Sci. Transl. Med. 9 (373), eaal2144.
Fuller, M.J., et al., 2004. Maintenance, loss, and resurgence of T cell responses during acute, protracted, and chronic viral infections. J. Immunol. 172 (7), 4204–4214.
Gaebler, C., et al., 2022. Prolonged viral suppression with anti-HIV-1 antibody therapy. Nature 606 (7913), 368–374.
Gray, E.S., et al., 2011. The neutralization breadth of HIV-1 develops incrementally over four years and is associated with CD4+ T cell decline and high viral load during acute infection. J. Virol. 85 (10), 4828–4840.
Gulick, R.M., et al., 1997. Treatment with indinavir, zidovudine, and lamivudine in adults with human immunodeficiency virus infection and prior antiretroviral therapy. N. Engl. J. Med. 337 (11), 734–739.
Guo, A.-L., et al., 2022. Implications of the accumulation of CXCR5+ NK cells in lymph nodes of HIV-1 infected patients. EBioMedicine 75.
Halper-Stromberg, A., et al., 2014. Broadly neutralizing antibodies and viral inducers decrease rebound from HIV-1 latent reservoirs in humanized mice. Cell 158 (5), 989–999.
Hammer, S.M., et al., 1997. A controlled trial of two nucleoside analogues plus indinavir in persons with human immunodeficiency virus infection and CD4 cell counts of 200 per cubic millimeter or less. N. Engl. J. Med. 337 (11), 725–733.
Hartana, C.A., et al., 2022. Immune correlates of HIV-1 reservoir cell decline in early-treated infants. Cell Rep. 40 (3).
Hartana, C.A., et al., 2023. IL-15-dependent immune crosstalk between natural killer cells and dendritic cells in HIV-1 elite controllers. Cell Rep. 42 (12).
Hayes, J.M., et al., 2014. Fc gamma receptor glycosylation modulates the binding of IgG glycoforms: a requirement for stable antibody interactions. J. Proteome Res. 13 (12), 5471–5485.

Hill, A.L., et al., 2014. Predicting the outcomes of treatment to eradicate the latent reservoir for HIV-1. Proc. Natl. Acad. Sci. USA 111 (37), 13475–13480.
Horwitz, J.A., et al., 2013. HIV-1 suppression and durable control by combining single broadly neutralizing antibodies and antiretroviral drugs in humanized mice. Proc. Natl. Acad. Sci. USA 110 (41), 16538–16543.
Hraber, P., et al., 2014. Prevalence of broadly neutralizing antibody responses during chronic HIV-1 infection. AIDS 28 (2), 163 (London, England).
Hua, S., et al., 2018. Pegylated interferon-α–induced natural killer cell activation is associated with human immunodeficiency virus-1 DNA decline in antiretroviral therapy–treated HIV-1/Hepatitis C virus–coinfected patients. Clin. Infect. Dis. 66 (12), 1910–1917.
Klein, F., et al., 2012. HIV therapy by a combination of broadly neutralizing antibodies in humanized mice. Nature 492 (7427), 118–122.
Kumar, S., Singh, S., Luthra, K., 2023. An overview of human anti-HIV-1 neutralizing antibodies against diverse epitopes of HIV-1. ACS Omega.
Lazar, G.A., et al., 2006. Engineered antibody Fc variants with enhanced effector function. Proc. Natl. Acad. Sci. USA 103 (11), 4005–4010.
Lewis, G.K., et al., 2019. Knowns and unknowns of assaying antibody-dependent cell-mediated cytotoxicity against HIV-1. Front. Immunol. 10, 1025.
Liu, S.D., et al., 2015. Afucosylated antibodies increase activation of FcγRIIIa-dependent signaling components to intensify processes promoting ADCC. Cancer Immunol. Res. 3 (2), 173–183.
Liu, Y., et al., 2020a. Broadly neutralizing antibodies for HIV-1: efficacies, challenges and opportunities. Emerg. Microb. Infect. 9 (1), 194–206.
Liu, R., et al., 2020b. Fc-engineering for modulated effector functions—improving antibodies for cancer treatment. Antibodies 9 (4), 64.
Lu, C.-L., et al., 2016. Enhanced clearance of HIV-1–infected cells by broadly neutralizing antibodies against HIV-1 in vivo. Science 352 (6288), 1001–1004.
Mackness, B.C., et al., 2019. Antibody Fc engineering for enhanced neonatal Fc receptor binding and prolonged circulation half-life. In: MAbs. Taylor & Francis.
Maldarelli, F., et al., 2014. Specific HIV integration sites are linked to clonal expansion and persistence of infected cells. Science 345 (6193), 179–183.
Marchitto, L., et al., 2023. Impact of HIV-1 Vpu-mediated downregulation of CD48 on NK-cell-mediated antibody-dependent cellular cytotoxicity. mBio 14 (4), e00789.
Mendoza, P., et al., 2018. Combination therapy with anti-HIV-1 antibodies maintains viral suppression. Nature 561 (7724), 479–484.
Mikulak, J., et al., 2017. Natural killer cells in HIV-1 infection and therapy. AIDS 31 (17), 2317–2330.
Moyo-Gwete, T., et al., 2022. Enhanced neutralization potency of an identical HIV neutralizing antibody expressed as different isotypes is achieved through genetically distinct mechanisms. Sci. Rep. 12 (1), 16473.
Naranjo-Gomez, M., Pelegrin, M., 2023. Vaccinal effect of HIV-1 antibody therapy: dream or reality? Curr. Opin. HIV AIDS 18 (4), 209–216.
Niessl, J., et al., 2020. Combination anti-HIV-1 antibody therapy is associated with increased virus-specific T cell immunity. Nat. Med. 26 (2), 222–227.
Nimmerjahn, F., Ravetch, J.V., 2006. Fcγ receptors: old friends and new family members. Immunity 24 (1), 19–28.
Nishimura, Y., et al., 2017. Early antibody therapy can induce long-lasting immunity to SHIV. Nature 543 (7646), 559–563.
Niwa, R., et al., 2004. Enhancement of the antibody-dependent cellular cytotoxicity of low-fucose IgG1 is independent of FcγRIIIa functional polymorphism. Clin. Cancer Res. 10 (18), 6248–6255.
Olesen, R., et al., 2015. Innate immune activity correlates with CD4 T cell-associated HIV-1 DNA decline during latency-reversing treatment with panobinostat. J. Virol. 89 (20), 10176–10189.
Pace, M., et al., 2022. Impact of antiretroviral therapy in primary HIV infection on natural killer cell function and the association with viral rebound and HIV DNA following treatment interruption. Front. Immunol. 13, 878743.
Pierson, T., McArthur, J., Siliciano, R.F., 2000. Reservoirs for HIV-1: mechanisms for viral persistence in the presence of antiviral immune responses and antiretroviral therapy. Annu. Rev. Immunol. 18 (1), 665–708.
Plomp, R., et al., 2015. Hinge-region O-glycosylation of human immunoglobulin G3 (IgG3)*[S]. Mol. Cell. Proteomics 14 (5), 1373–1384.
Redpath, S., et al., 1998. The influence of the hinge region length in binding of human IgG to human Fcγ receptors. Hum. Immunol. 59 (11), 720–727.
Ren, Y., et al., 2020. Relationships between neutralization, binding, and ADCC of broadly neutralizing antibodies against reservoir HIV. J. Virol. 95 (2). https://doi.org/10.1128/jvi.0180820.
Repp, R., et al., 2011. Combined Fc-protein-and Fc-glyco-engineering of scFv-Fc fusion proteins synergistically enhances CD16a binding but does not further enhance NK-cell mediated ADCC. J. Immunol. Methods 373 (1–2), 67–78.
Richard, J., et al., 2018. Uninfected bystander cells impact the measurement of HIV-specific antibody-dependent cellular cytotoxicity responses. mBio 9, e00358. PMID: 29559570587491310.1128/mBio.
Richard, J., et al., 2021. Across functional boundaries: making nonneutralizing antibodies to neutralize HIV-1 and mediate Fc-mediated effector killing of infected cells. mBio 12 (5). https://doi.org/10.1128/mbio.0140521.
Richards, J.O., et al., 2008. Optimization of antibody binding to FcγRIIa enhances macrophage phagocytosis of tumor cells. Mol. Cancer Therapeut. 7 (8), 2517–2527.
Richardson, S.I., et al., 2019. IgG3 enhances neutralization potency and Fc effector function of an HIV V2-specific broadly neutralizing antibody. PLoS Pathog. 15 (12), e1008064.
Richardson, S.I., et al., 2021. HIV broadly neutralizing antibodies expressed as IgG3 preserve neutralization potency and show improved Fc effector function. Front. Immunol. 3620.
Robinson, J.I., et al., 2018. Affimer proteins inhibit immune complex binding to FcγRIIIa with high specificity through competitive and allosteric modes of action. Proc. Natl. Acad. Sci. USA 115 (1), E72–E81.
Rosás-Umbert, M., et al., 2022. Administration of broadly neutralizing anti-HIV-1 antibodies at ART initiation maintains long-term CD8+ T cell immunity. Nat. Commun. 13 (1), 6473.
Saxena, A., Wu, D., 2016. Advances in therapeutic Fc engineering–modulation of IgG-associated effector functions and serum half-life. Front. Immunol. 7, 580.
Scheid, J.F., et al., 2009. Broad diversity of neutralizing antibodies isolated from memory B cells in HIV-infected individuals. Nature 458 (7238), 636–640.
Schlothauer, T., et al., 2016. Novel human IgG1 and IgG4 Fc-engineered antibodies with completely abolished immune effector functions. Protein Eng. Des. Sel. 29 (10), 457–466.
Schoofs, T., et al., 2016. HIV-1 therapy with monoclonal antibody 3BNC117 elicits host immune responses against HIV-1. Science 352 (6288), 997–1001.
Schriek, A.I., et al., 2022. Anti-HIV-1 nanobody-IgG1 constructs with improved neutralization potency and the ability to mediate Fc effector functions. Front. Immunol. 13.
Schriek, A., et al., 2023. Next-generation bNAbs for HIV-1 cure strategies. Antivir. Res., 105788
Shingai, M., et al., 2013. Antibody-mediated immunotherapy of macaques chronically infected with SHIV suppresses viraemia. Nature 503 (7475), 277–280.
Smith, J.A., Daniel, R., 2006. Following the path of the virus: the exploitation of host DNA repair mechanisms by retroviruses. ACS Chem. Biol. 1 (4), 217–226.
Sneller, M.C., et al., 2022. Combination anti-HIV antibodies provide sustained virological suppression. Nature 1–7.
Sok, D., Burton, D.R., 2018. Recent progress in broadly neutralizing antibodies to HIV. Nat. Immunol. 19 (11), 1179–1188.
Stavenhagen, J.B., et al., 2007. Fc optimization of therapeutic antibodies enhances their ability to kill tumor cells in vitro and controls tumor expansion in vivo via low-affinity activating Fcγ receptors. Cancer Res. 67 (18), 8882–8890.
Suryawanshi, P., et al., 2021. Anti-HIV-1 ADCC and HIV-1 env can be partners in reducing latent HIV reservoir. Front. Immunol. 12, 663919.
De Taeye, S.W., et al., 2020. FcγR binding and ADCC activity of human IgG allotypes. Front. Immunol. 11, 740.
de Taeye, S.W., et al., 2024. Afucosylated broadly neutralizing antibodies enhance clearance of HIV-1 infected cells through cell-mediated killing. Commun. Biol. 7 (1), 964.
Tridandapani, S., et al., 2002. Regulated expression and inhibitory function of FcγRIIb in human monocytic cells. J. Biol. Chem. 277 (7), 5082–5089.
Tuyishime, M., et al., 2020. Improved killing of HIV-infected cells using three neutralizing and non-neutralizing antibodies. J. Clin. Invest. 130 (10), 5157–5170.
Utay, N.S., et al., 2020. Timing of antiretroviral therapy initiation determines rectal natural killer cell populations. AIDS Res. Hum. Retrovir. 36 (4), 314–323.
Vidarsson, G., Dekkers, G., Rispens, T., 2014. IgG subclasses and allotypes: from structure to effector functions. Front. Immunol. 5, 520.
Wagner, T.A., et al., 2014. Proliferation of cells with HIV integrated into cancer genes contributes to persistent infection. Science 345 (6196), 570–573.
Wines, B.D., et al., 2016. Dimeric FcγR ectodomains as probes of the Fc receptor function of anti-influenza virus IgG. J. Immunol. 197 (4), 1507–1516.
Zhao, C., et al., 2022. The HIV Env glycoprotein conformational states on cells and viruses. mBio 13 (2), e01825.
Zhong, X., et al., 2022. Impacts of fast production of afucosylated antibodies and Fc mutants in ExpiCHO-S™ for enhancing FcγRIIIa binding and NK cell activation. J. Biotechnol. 360, 79–91.